# Evidence for Different Ferromagnetic Phases in Amorphous $Fe_{40}Ni_{40}B_{20}$ Detected by EPR

R. Gerling

GKSS-Forschungszentrum, Institut für Physik

K. Dräger

Institut für Physikalische Chemie der Universität Hamburg

Z. Naturforsch. **38 a**, 20–26 (1983); received November 6, 1982

Amorphous ferromagnetic $Fe_{40}Ni_{40}B_{20}$ ($T_c = 662$ K) has been investigated by EPR in the temperature range from 110 to 510 K. From the temperature dependence of the magnetic field at resonance, the saturation magnetization could be evaluated. Around 470 K the line width of the resonance signal exhibits a pronounced minimum, and the EPR-intensity deviates at this temperature from pure ferromagnetic behaviour. Both effects can be explained by assuming the presence of a second ferromagnetic phase with a Curie temperature of $T_c' = 470$ K. Upon annealing of $Fe_{40}Ni_{40}B_{20}$ at temperatures slightly higher than $T_c'$ changes in physical properties, such as Curie temperature, density and relative strain at fracture are observable. It is proposed that the onset of the low temperature relaxation which is responsible for these changes in physical properties is related to the transition of the second ferromagnetic phase to the paramagnetic state.

## 1. Introduction

One of several possible methods for the production of amorphous metals is the single roller quenching process. Ribbons produced by this technique always exhibit a dull and a bright side. Investigations have revealed several physical properties to be quite different with respect to regions near to the two surfaces [1–3]. The reason for the different behaviour is thought to be due to the different thermal history of the two sides. The dull side was in contact with the roller during the quenching, and thus experienced a more rapid cooling rate than the bright side. Therefore, the two sides are in different states of relaxation and as shown by Nagy et al. [3] for several B-containing glasses, there are even differences in the B-concentration with respect to the near-surface regions of the two sides. An amorphous ribbon produced by the single roller quenching like the ribbon used by us, can therefore not be regarded as being homogeneous on the scale of its thickness. As recently reported, there is further evidence that the ribbons are inhomogeneous on a still smaller scale. Atom-probe field ion microscopy (FIM) on $Fe_{40}Ni_{40}B_{20}$ by Piller et al. [4] revealed fluctuations in the chemical composition in the as-quenched state due to boron rich precipitates in a B-depleted matrix. The radius of the precipitates was about 1.5 nm and the B-concentration about 25 at-%. By small angle X-ray scattering (SMAXS) Osamura et al. [5] concluded that the structure of Fe-B amorphous alloys can be described as being closely related to a dual structure of $Fe_3B$ and Fe. Besides chemical inhomogeneities as reported by these authors, computer simulations of the amorphous structure by Egami et al. [6] revealed different topological inhomogeneities also to exist in rapidly quenched metals. These topological inhomogeneities can be described by p- and n-type defects which are more and less dense regions with respect to the average density of the amorphous alloy. In order to obtain more information about these inhomogeneities on a very small scale, experimental techniques which are sensitive to changes in the neighborhood of single atoms are required. One of these methods is the electron paramagnetic resonance (EPR), as this technique is very sensitive to the magnetic interaction of single atoms with their nearest neighbors. In order to confirm present conceptions concerning the homogeneity of amorphous alloys we have performed temperature dependent EPR-measurements on as-quenched $Fe_{40}Ni_{40}B_{20}$ specimens. Special attention has been paid to the covered temperature range in order to avoid relaxation to take place during the measurements, as well as to avoid an influence of the change of properties near $T_c$ ($\sim 662$ K) to which EPR-experiments are highly sensitive.

Reprint requests to Dr. R. Gerling, GKSS-Forschungszentrum, Institut für Physik, Box 1160, D-2054 Geesthacht, FRG.

0340-4811 / 83 / 0100-0020 $ 01.3 0/0. – Please order a reprint rather than making your own copy.

Dieses Werk wurde im Jahr 2013 vom Verlag Zeitschrift für Naturforschung in Zusammenarbeit mit der Max-Planck-Gesellschaft zur Förderung der Wissenschaften e.V. digitalisiert und unter folgender Lizenz veröffentlicht: Creative Commons Namensnennung-Keine Bearbeitung 3.0 Deutschland Lizenz.

This work has been digitalized and published in 2013 by Verlag Zeitschrift für Naturforschung in cooperation with the Max Planck Society for the Advancement of Science under a Creative Commons Attribution-NoDerivs 3.0 Germany License.

Zum 01.01.2015 ist eine Anpassung der Lizenzbedingungen (Entfall der Creative Commons Lizenzbedingung „Keine Bearbeitung") beabsichtigt, um eine Nachnutzung auch im Rahmen zukünftiger wissenschaftlicher Nutzungsformen zu ermöglichen.

On 01.01.2015 it is planned to change the License Conditions (the removal of the Creative Commons License condition "no derivative works"). This is to allow reuse in the area of future scientific usage.

## 2. Experimental

$Fe_{40}Ni_{40}B_{20}$ (0040 Vitrovac, Vakuumschmelze Hanau, FRG) about 5 mm wide and 50 μm thick has been used for our experiments. Specimens of $2 \times 5$ mm$^2$ were cut from the ribbon. Both the shiny and the dull side were removed by electropolishing. The resonance experiments were performed on a Bruker EPR spectrometer, x-band at $\nu = 9.3$ GHz. The temperature of the specimens inside a quartz dewar could be varied over the range from 130 to 510 K with an accuracy of ~ 0.5 K. During the experiments the amorphous material was exposed to a pure nitrogen atmosphere. Prior to the start of the EPR-experiments, each specimen was kept for 30 min at a temperature of 510 K. The measurement was then started at 510 K, and after each run the temperature was lowered in steps of ~ 20 K. Because of the anisotropy of the magnetic properties the position and alignment of the amorphous specimens inside the resonator with respect to the applied external field has to be well defined and kept unchanged during the whole experiment. In order to describe the alignment of the samples, the geometry of the specimens may be characterized by two vectors. The first one, ***a*** points along the direction of the as-quenched ribbon, whereas ***c*** is chosen as the normal vector of the shiny surface of the ribbon (Fig. 1).

Small pieces of the ribbon were examined in two specific positions with respect to the applied external field: (i) called the parallel orientation with $\boldsymbol{a} \parallel \boldsymbol{H}$ and $\boldsymbol{c} \perp \boldsymbol{H}$ and (ii) the perpendicular orientation with $\boldsymbol{a} \perp \boldsymbol{H}$ and $\boldsymbol{c} \parallel \boldsymbol{H}$. The two orientations exhibited great differences in their resonance behaviour, especially with respect to the strength of the magnetic field at resonance and the intensity of absorption.

Figure 2 shows the EPR absorption signal at room temperature for the parallel orientation. The resonance signal results from a field sweep of $\dot{H} = 400$ G/min. In addition, specimens of the same material have been heat-treated in evacuated, sealed capsules for 43 h at temperatures from 430 to 530 K. After this treatment the specimens were investigated by several methods. Differential scanning calorimetry (Perkin Elmer DSC-2) has been performed in order to determine the crystallization temperature and enthalpy (scanning rate 20 K/min), as well as to measure the Curie temperature (scanning rate 40 K/min). The relative strain at fracture, $\varepsilon_f$, could be evaluated from simple bending tests [7]. The densities of the differently treated specimens were determined by weighing foils ($35 \times 15 \times 0.04$ mm$^3$) in both air and tetrabromoethane using a magnetic suspension balance.

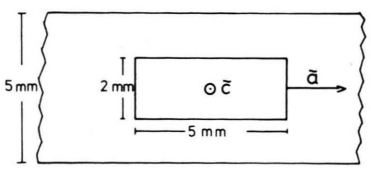


Fig. 1. Schematic drawing showing the geometry and orientation of the EPR-specimens. The vector ***a*** points along the direction of the ribbon, ***c*** is the normal vector to the shiny side. The orientation of ***H*** is restricted to the plane given by the two vectors ***a*** and ***c***.

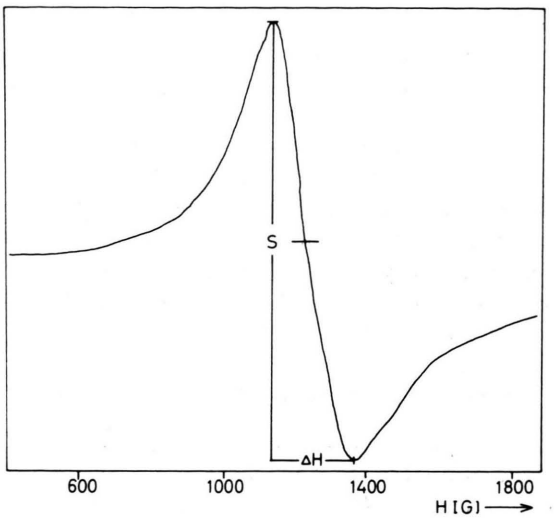


Fig. 2. EPR absorption signal at room temperature for the parallel orientation ($\boldsymbol{a} \parallel \boldsymbol{H}$ and $\boldsymbol{c} \perp \boldsymbol{H}$).

## 3. Results

### *3.1 Differential Scanning Calorimetry, Bending Tests and Density Measurements*

The crystallization temperature $T_x$ and the crystallization enthalpy $H_c$ did not reveal any difference for all the differently heat treated specimens with respect to the as-quenched material; $T_x = 714$ K, $H_c = 24.5$ cal/g. The change of the Curie temperature is shown in Figure 3. $T_c$ increases continuously to about $\Delta T_c = 0.25$ K for the highest annealing temperature of 530 K. The density exhibits a more step-

like behaviour (Fig. 3) and changes by about 0.1% at 460 K. Although the experimental error in $\varrho$ is rather large with respect to the small changes, but as the thermal dilatation experiments by Kursumovic et al. [8] on the same material revealed a peculiar contraction at about 460 K, the step-like behaviour of $\varrho$ indeed is realistic. The most significant changes are seen in the relative strain at fracture (Figure 3). For temperatures beyond 430 K, $\varepsilon_f$ decreases sharply to about $\varepsilon_f = 2 \cdot 10^{-2}$ after 43 h at 470 K. With further increasing temperature $\varepsilon_f$ stays constant.

### 3.2 *Temperature Dependence of the Resonance Field*

The temperature dependence of the resonance field for the orientation $\boldsymbol{a} \parallel \boldsymbol{H}$ is shown in Figure 4. Over the whole range $H_\parallel$ increases with increasing temperature. As in this case the orientation of the specimen is parallel to the easy direction of magnetization $\boldsymbol{M}_s$, it is necessary to take account of the specific influence on the resonance event. With $\omega$ called the Lamour frequency, Kittel [9] deduced the resonance equation,

$$\omega^2 = \gamma^2 H_\parallel [H_\parallel + 4\pi M_s] \tag{1}$$

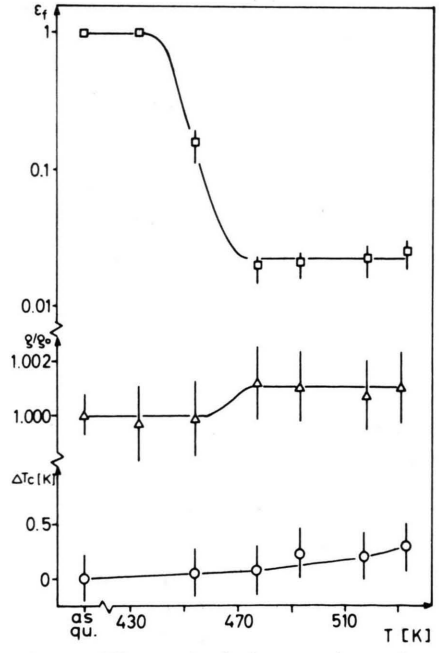


Fig. 3. Different physical properties as the relative strain at fracture $\varepsilon_f$ (□), relative density $\varrho/\varrho_0$ (△) and the change of the Curie temperature $\Delta T_c$ (○) for specimens heat treated for 43 h at the respective temperature.

with $\gamma = g\,\mu_B/\hbar$. However, (1) is applicable only to homogeneous ferromagnetic materials. Nevertheless we consider this condition to be fulfilled by amorphous metals. The influence of $T$ on $M_s$ was then calculated with $g = 2.003$ using (1) for all temperatures. The results are plotted in Figure 4. With increasing temperature the decrease of $M_s$ exhibits the well known behaviour for ferromagnetic materials. For the perpendicular orientation ($\boldsymbol{H} \perp \boldsymbol{a}$ and $\boldsymbol{c} \parallel \boldsymbol{H}$), (1) has to be replaced by

$$\omega = \gamma [H_\perp - 4\pi M_s]\,. \tag{2}$$

In our case the resonance signal then should be detectable at about $H_\perp = 13000$ G. Because of the restricted field-range of the spectrometer, this resonance signal was beyond our possibilities. However, in the lower field-range ($\sim 500$ G), a further resonance absorption could be observed. The $T$-dependence of its magnetic field $H_\perp$ is shown in Figure 5. With increasing temperature $H_\perp$ decreases continuously.

### 3.3 *The Temperature Dependence of the EPR Intensity*

For the parallel orientation, the line width $\Delta H$ as well as the height $S$ of the resonance signal are shown in Figure 6. With increasing temperature $\Delta H$ exhibits a slight decrease up to 310 K, followed by a more pronounced decrease between 310 and 425 K. At 465 K $\Delta H$ passes through a minimum and increases sharply with further increasing temperature. The signal height $S$ exhibits a complementary behaviour.

As our spectrometer recorded the first derivative of the resonance signal, the absorption intensity can be computed from

$$I^* = K S\, \Delta H^2, \tag{3}$$

where $S$ and $\Delta H$ are the signal height and line width, respectively; $K$ represents a shape-factor of the line. Since the line shape did not change significantly over the whole temperature range, $K$ may be considered as a constant. Moreover, as only relative values are of interest with respect to a fixed temperature $T_0$, the relative intensity may be evaluated from

$$I(T) = \frac{S(T)\,\Delta H(T)^2}{S(T_0)\,\Delta H(T_0)^2}. \tag{4}$$

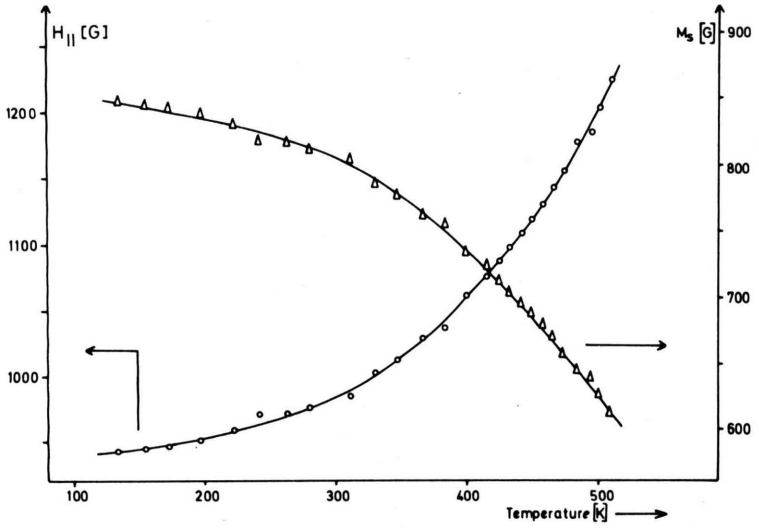


Fig. 4. The temperature dependence of the strength of the magnetic field at resonance (○) for the parallel orientation and the saturation magnetization (△) as calculated from Eq. (1).

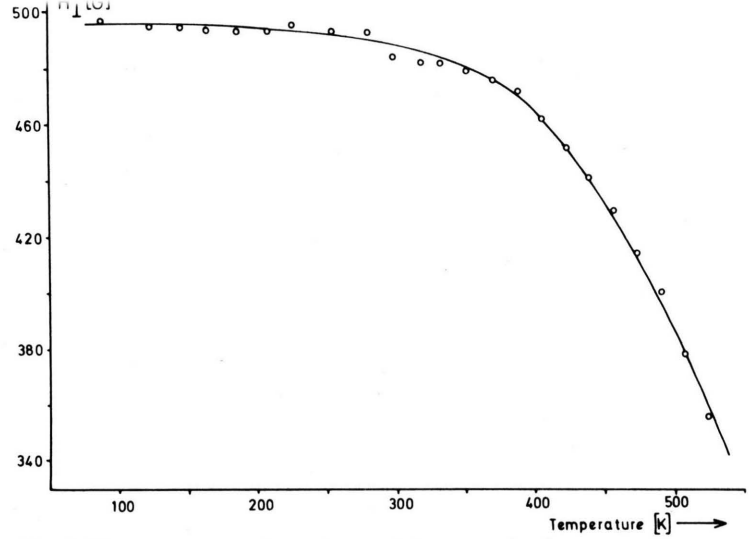


Fig. 5. The temperature dependence of the strength of the magnetic field at resonance for the perpendicular orientation.

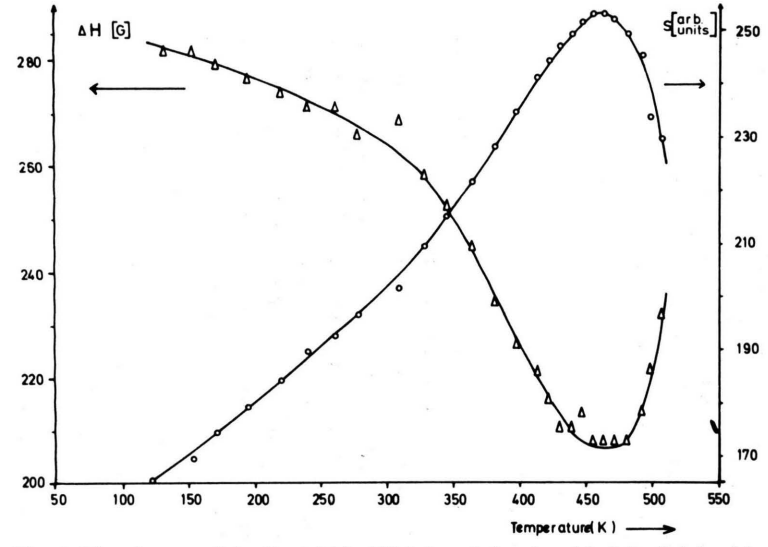


Fig. 6. The change of the linewidth $\Delta H$ (△) and the signal height $S$ (○) with the temperature. Orientation: $\boldsymbol{a} \parallel \boldsymbol{H}$; $\boldsymbol{c} \perp \boldsymbol{H}$.

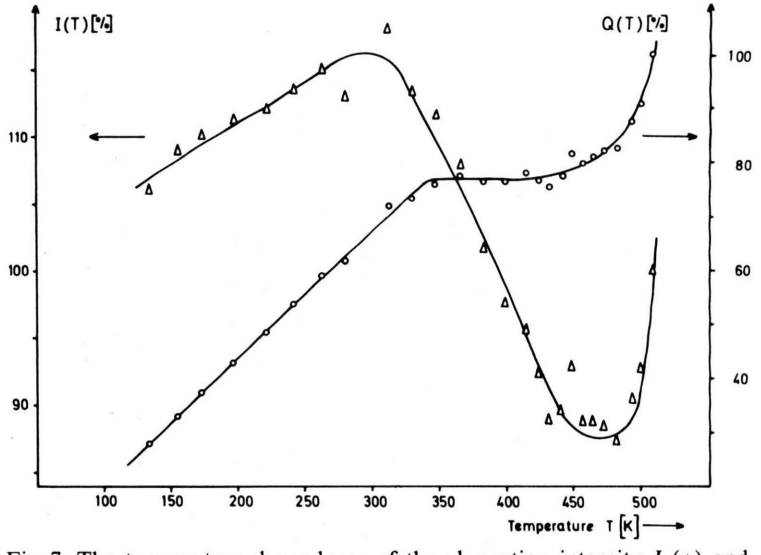


Fig. 7. The temperature dependence of the absorption intensity $I$ (△) and the reduced intensity $Q$ (○) for the parallel orientation. $I$ has been calculated from (4) and $Q$ from (5).

In order to discuss the non-paramagnetic effect of the resonance absorption, it is useful to introduce a function $Q(T)$ as the reduced intensity given by

$$Q(T) = \frac{I(T)\,T}{I(T_0)\,T_0}. \tag{5}$$

Its advantage can be seen from the following example. In paramagnetic materials, the absorption intensity $I$ is proportional to $T^{-1}$ [10] and thus the reduced intensity $Q$ will be a constant with respect to the temperature. Both the intensity and the reduced intensity are shown in Figure 7. The behaviour of $I$ may be subdivided into three temperature intervals. From 110 to 300 K the intensity increases, which is largely due to the increase in $S$ of $\sim 23\%$, while $\Delta H$, although squared in (4), decreases in this range by only 6%. The maximum of $I$ at 300 K and its subsequent decrease coincides with the enhanced decreases of $\Delta H$ in this range. The minimum of $I$ at 465 K coincides with the extrema of $\Delta H$ and $S$. The final sharp increase of $I$ above 470 K is chiefly due to the pronounced increase of $\Delta H$. With the application of the function $Q$ the effect of the sample temperature on the EPR-parameters is taken into account, therefore the dependence of $Q$ on $T$ is quite different from that of $I$. The slight increase of $Q$ from 110 to 340 K is followed by a plateau between 340 and 420 K. Beyond 420 K a further increase can be detected which is more pronounced than between 110 and 340 K.

## 4. Discussion

As rapidly quenched amorphous metals like $Fe_{40}Ni_{40}B_{20}$ are metastable with respect to the fully crystallized material of the same composition, these amorphous alloys tend to relax or even crystallize upon heating. For temperature dependent investigations like these EPR-measurements the temperature range as well as the time for each measurement must be carefully chosen in order to avoid the possibility that any relaxation occurs during the experiments. Such a relaxation would alter the properties of the amorphous metal and thus might either conceal or produce a measureable effect. In the case of amorphous $Fe_{40}Ni_{40}B_{20}$ the effects of irreversible low temperature relaxations are well known [4, 8]. Changes of some physical properties are shown in Figure 3. One of the most sensitive physical properties to low temperature relaxation is the relative strain at fracture. After annealing 43 h at the highest temperature for the EPR experiments (510 K) specimens were found to be brittle. As reported by Piller et al. [4] thermal treatment of $Fe_{40}Ni_{40}B_{20}$ at 520 K for only 5 h did not alter the relative strain at fracture. We therefore conclude that although irreversible structural relaxation does occur even at temperatures around 500 K as indicated by the physical property changes shown in Fig. 3, we can rule out a relaxation of the EPR-specimens as they were kept for only 30 min at these elevated temperatures.

The increase of the resonance field $H_\parallel$ with increasing temperature in the case of the parallel orientation (Fig. 4) can be explained by the ferromagnetism of the specimen. In the same temperature range the decrease of $H_\perp$ in the case of the perpendicular orientation is in accordance with the predictions of (2). As, in general, the magnetization $M_s$ decreases with increasing temperature, the decrease of $H_\perp$ can be interpreted as a consequence of ferromagnetism, although the strength of the resonance field remains unclear at present.

The calculation with the aid of (1) reveals the magnetization at room temperature to be $4\pi M_s = 10130 \pm 150$ G. This is in good agreement with Becker et al. [11] and O'Handly et al. [12], who found values for $4\pi M_s$ for $Fe_{40}Ni_{40}B_{20}$ at room temperature of 10420 and 10000 G, respectively. As both authors applied a static method to determine the magnetization, the good agreement with our result justifies the assumption that $Fe_{40}Ni_{40}B_{20}$ can be considered a homogeneous ferromagnetic material in the sense of (1). Indeed by electropolishing the EPR-specimens the regions near the both surfaces of the as-quenched ribbon have been removed with the result that inhomogeneities due to the B-concentration fluctuations at the surface as reported by Nagy et al. [3] were no longer present. The material therefore should tend to exhibit a better homogeneity with respect to the unprepared as-quenched ribbon. However, it must be pointed out that the magnetization is determined by the density of magnetic moments and is therefore a local quantity. Since $M_s$ from (1) represents the mean value of this quantity over the volume of the whole specimen it should not be sensitive to inhomogeneities on a much smaller scale. Thus,

further information can only be extracted from those EPR-parameters which are sensitive to local fluctuations. In contrast to the smooth temperature dependence of $M_s$, the line width and the height of the signal reflect these properties and exhibit significant extrema. Special attention must be paid to the minimum of $\Delta H$, because this result is not expected to be found in a homogeneous ferromagnetic material. As was shown by Vonsovskii [13] and Bagguley et al. [14] $\Delta H$ decreases continuously with increasing temperature provided $T < T_c$. This behaviour indeed has been detected for $Fe_{40}Ni_{40}B_{20}$ by Petterson et al. [15] who reported that in the range from 100 to 600 K there is a general decrease of $\Delta H$. Our detailed investigations in a smaller temperature range and with a better resolution of the linewidth, however, have allowed the anomaly in $\Delta H$ around 465 K, which is still far below the Curie temperature of the bulk material ($T_c = 662$ K) to be observed. The minimum of $\Delta H$ may be explained by the existence of at least a second ferromagnetic phase [SFP] which is characterized by a Curie temperature of $T_c' = 470$ K.

A system of two ferromagnetic phases with different Curie temperatures has magnetic properties which are consistent with the anormal behaviour of $\Delta H$ as shown in Figure 6. The assumption of an SFP with $T_c' = 470$ K would predict a steep increase of the linewidth for temperatures $T > T_c'$ as a consequence of its change to paramagnetism [13], and the experimental results support this interpretation. The assumption of an SFP is also compatible with the temperature dependence of the ESR-intensity and the reduced intensity $Q$. Figure 7 shows an increase of $Q$ with increasing temperature up to 350 K. This behaviour is an effect of the growing density of collective spin-states that will be occupied at higher temperatures only. Between 350 and 475 K, however, $Q$ exhibits a more constant behaviour. This may be understood if we recall that in the SFP the cooperative interaction will break down in the vicinity of the transition temperature $T_c'$. As a consequence the number of occupied spin-states will not grow longer. This applies to the SFP, whilst the bulk material remains ferromagnetic. As the measurement reveals an overlap of both effects the result is that the reduced intensity $Q$ remains constant in this range of temperature. For higher temperatures ($T > T_c'$) the bulk material determines the magnetic behaviour of the specimen, hence the reduced intensity $Q$ continues to increase. Figure 7 shows this effect for $T > 475$ K. The volume fraction occupied by the SFP cannot, however, be determined from these experiments. Nevertheless, from the smooth continuous decrease of $M_s$, it may be concluded that the volume fraction of this phase is indeed rather small.

Some recent investigations on $Fe_{40}Ni_{40}B_{20}$ and Fe-B amorphous alloys have revealed that besides the above mentioned chemical inhomogeneities in near-surface regions, there are additional compositional inhomogeneities inside the amorphous ribbon. By means of atom probe FIM Piller et al. [4] found in $Fe_{40}Ni_{40}B_{20}$ amorphous precipitates enriched in the B-concentration to about 25%. These clusters of about 1.5 nm radius are embedded in a B-depleted matrix. Investigations by small angle X-ray scattering on Fe-B alloys by Osamura et al. [5] even revealed the glassy structure to be closely related to a dual structure of Fe and $Fe_3B$. On the basis of concentration fluctuations in the as-quenched amorphous alloys as well fluctuations in the (Fe, Ni) as in the (Fe, B) and (Ni, B) concentrations may be responsible for the SFP. As recently reported by Chien et al. [16] the Curie temperature of vapor deposited amorphous $Fe_{90}B_{10}$ is about 470 K. On the other hand to explain the observed $T_c'$ by (Fe, Ni) compositional fluctuations, a decomposition to $(Fe_{0.3}Ni_{0.7})_{80}B_{20}$, is necessary [11, 17]. As these two examples show, high amplitudes of the concentration fluctuations would be necessary to form a SFP with a Curie temperature of about 470 K. But because of the short ranges of the magnetic interactions in general the Curie temperature will result from the contribution of the next nearest neighbors only. Thus, the required high amplitudes of the concentration fluctuations can be restricted to very small volumes.

Besides chemical inhomogeneities possibly topological defects may cause the SFP. Computer models of amorphous metals have revealed topological defects called p- and n-type defects to exist within the amorphous matrix [6]. In this context discussed here the n-type defects are the more interesting ones. Since they are less dense regions which contain a large amount of the excess volume, the distances between the atoms forming this type of defect are slightly larger with respect to those in the matrix. As the strength of the magnetic interaction varies strongly with the distance between the inter-

acting atoms, the magnetic coupling is diminished in the n-defects and the Curie temperature would be reduced with respect to the matrix. Following these considerations, the n-type defects could be associated directly with the SFP. However, at present it cannot be decided whether the SFP is caused rather by topological or chemical inhomogeneities.

Thermal dilatation measurements on $Fe_{40}Ni_{40}B_{20}$ performed by Kursomovic et al. [8] have revealed peculiar contractions of the ribbon at 460 and 570 K, as well as at the "final" Curie temperature of 662 K. The contractions at 460 and 570 K have been attributed by the authors as being due to thermally-induced structural relaxation. Indeed the length change at 460 K coincides with the Curie temperature of the SFP. Moreover, the second contraction may even be due to a third ferromagnetic phase. The observed changes of several physical properties as shown in Fig. 3 after heating $Fe_{40}Ni_{40}B_{20}$ for 43 h at different temperatures may then be interpreted in terms of the structural relaxation which should start at about 460 K. As this temperature coincides with $T_c'$ of the SFP from the present work, the magnetic transition of the second ferromagnetic phase indeed may initiate the onset of the structural relaxation.

[1] A. L. Greer and J. A. Leake, Rapidly Quenched Metals III, The Metals Society, London 1978, Vol. 1, p. 299.
[2] A. S. Schaafsma, H. Snijders, and F. van der Woude, Phys. Rev. B **20,** 4423 (1979).
[3] A. Z. Nagy, B. Vasvari, P. Duwez, L. Bakos, J. Bogancs, and V. M. Nazarov, phys. stat. sol. (a) **61,** 689 (1980).
[4] J. Piller and P. Haasen, Acta Met. **30,** 1 (1982).
[5] K. Osamura. R. Suzuki, and Y. Murakami, Rapidly Quenched Metals, The Japan Institute of Metals, Sendai 1982, Vol. 1, p. 431.
[6] T. Egami, K. Maeda, and V. Vitek, Phil. Mag. A **41,** 883 (1980).
[7] R. Gerling and R. Wagner, Journ. Nucl. Mater. **107,** 311 (1982).
[8] A. Kursumovic, E. Girt, E. Babic, B. Leontic, and N. Njuhovic, Journ. Non-Cryst. solids **44,** 57 (1981).
[9] C. Kittel, Phys. Rev. **71,** 270 (1947); **73,** 155 (1948).
[10] A. Abragam and B. Bleaney, Electron Paramagnetic Resonance of Transition Ions, Clarendon Press, Oxford 1970, p. 119.
[11] J. J. Becker, F. E. Luborsky, and J. L. Walter, IEEE Trans. Mag., MAG-13, 988 (1977).
[12] R. C. O'Handley, R. Hasegawa, R. Ray, and C. P. Chou, Appl. Phys. Letters **29,** 330 (1976).
[13] S. V. Vonsovskii, Ferromagnetic Resonance, Pergamon Press, New York 1966, p. 184.
[14] D. M. S. Bagguley and N. J. Harrick, Proc. Phys. Soc. A **67,** 648 (1954).
[15] L. Pettersson and S. Haraldson, Bull. Mag. Res. **2,** 282 (1980).
[16] C. L. Chien and K. M. Unruh, Phys. Rev. B **24,** 1556 (1981).
[17] S. Kouvel, Magnetism and Metallurgy, Academic Press, New York 1969, Vol. 2, p. 523.